An Intrusive Method for Two-Phase Flow under Uncertainty

By P. Pettersson, G. Iaccarino, K. K. So† AND C. Stemmer†

Center for Turbulence Research, Stanford University, 488 Escondido Mall
Stanford, CA 94305, USA

An intrusive stochastic projection method for two-phase time-dependent flows subject to uncertainty is presented. Numerical experiments are carried out assuming uncertainty in the interface location, but the framework generalizes to uncertainty with known distribution in other input data. Uncertainty is represented through generalized wavelet chaos expansion, and the system obtained from stochastic Galerkin projection is discretized in space with finite volume methods and flux limiting. The result is a robust solver that performs well for problems with sharp variation and discontinuities in the stochastic dimension. Experiments are assuming uncertainty in the interface location, but the framework generalizes to uncertainty with known distribution in other input data.

The numerical discretization of the governing equations is based on a generalization of the HLL flux, and have many properties in common with its deterministic counterpart. It is simple and robust, and captures the statistics of the shock. In a manner similar to the deterministic HLL solver, it does not capture the contact discontinuity, leading to an underestimate of the variance of the contact discontinuity.

1. Introduction

Physical models in computational fluid dynamics are often extended with stochastic models to represent uncertainty in governing equations or input parameters, including e.g. boundary and initial conditions, geometry and rates of reaction, diffusion and advection. One can distinguish between nonintrusive methods, where existing deterministic codes are run with a range of input values, and intrusive methods, where the problem is reformulated in a fashion that results in a modified problem that is larger than the original deterministic problem, but only needs to be solved once for the full solution of the stochastic problem. The increased complexity of the reformulated problem has the potential to reduce the computational cost compared to that of nonintrusive methods, such as Monte Carlo methods, that require numerous deterministic solutions, or stochastic numerical integration methods that require deterministic code solutions, evaluated at quadrature points in the stochastic dimension.

A stochastic two-phase problem in one spatial dimension is investigated as a first step towards developing an intrusive method for e.g. shock-bubble interaction with generic uncertainty in the input parameters. So *et al.* [1] investigated a two-dimensional two-phase problem subject to uncertainty in bubble deformation and contamination of

† Lehrstuhl für Aerodynamik und Strömungsmechanik, Technische Universität München, Boltzmannstr. 15, 85748 Garching b. München

the gas bubble, based on the experiments of [2]. The eccentricity of the elliptic bubble and the ratio of air-helium of the bubble were assumed to be random variables, and quantities of interest were obtained by numerical integration of the stochastic range (stochastic collocation). The problem selected here is inspired by this physical problem, and although we only study a one-dimensional problem, the future goal is to provide a formal comparison between the algorithm developed here and the non-intrusive techniques in [1].

We assume uncertainty in the location of the material interface, which requires a stochastic representation of all flow variables. Stochastic quantities are represented as generalized chaos series, that could be either global as in the case of generalized polynomial chaos [3], or localized, see e.g. [4]. For robustness, we use a generalized chaos expansion with Haar wavelets to represent the solution in the stochastic dimension [5]. It should be noted that this basis is global, so the method is fully intrusive. However, the basis is hierarchically localized in the sense that wavelets belonging to the same resolution level have non-overlapping support. These features makes it suitable for approximating discontinuities in the stochastic space without the oscillations that occur in the case of global polynomial bases.

The stochastic Galerkin method is applied to the stochastic two-phase formulation, resulting in a finite-dimensional deterministic system that shares many properties with the original deterministic problem. We assume that the stochastic Galerkin problem is hyperbolic. This generalized and extended two-phase problem is solved with the HLL-flux and MUSCL-reconstruction in space, and fourth order Runge-Kutta integration in time. The minmod flux limiter is employed in the experimental results displayed below.

2. Representation of uncertainty

The polynomial chaos framework for uncertainty quantification introduced by [6] and generalized by [3] is used to represent uncertainty in the input parameters of the governing equations.

Let ω be an outcome of a probability space $(\Omega, \mathcal{A}, P)$, with event space Ω, σ-algebra $\mathcal{A}$, and probability measure P. Let $\boldsymbol{\xi} = \{\xi_j(\omega)\}_{j=1}^{N}$ be a set of N i.i.d. random variables for $\omega \in \Omega$. Each random variable ξ_j is a mapping from the event space to $\mathbb{R}$. For the cases presented here, $N = 1$ i.e. a single source of uncertainty is assumed but the framework can be generalized to multiple sources of uncertainty.

Consider a generalized chaos basis $\{\Psi_i(\boldsymbol{\xi})\}_{i=0}^{\infty}$ spanning the space of second order (i.e. finite variance) random processes on this probability space. The basis functionals are assumed to be orthonormal,

$$\langle \Psi_i \Psi_j \rangle = \delta_{ij},$$

where δ_{ij} is the Kronecker delta and the inner product of $a(\xi(\omega))$ and $b(\xi(\omega))$ is defined by

$$\langle a(\xi(\omega))b(\xi(\omega)) \rangle = \int_{\Omega} a(\xi(\omega))b(\xi(\omega))dP(\omega).$$

Second order random fields $u(x, t, \xi)$ can be expressed as

$$u(x, t, \xi) = \sum_{i=0}^{\infty} u_i(x, t)\Psi_i(\xi). \tag{2.1}$$

Independent of the choice of orthogonal basis $\{\Psi_i\}_{i=0}^{\infty}$, we can express mean and vari-

ance of $u(x,t,\xi)$ as

$$E(u(x,t,\xi)) = u_0(x,t)$$

and

$$\mathrm{Var}(u(x,t,\xi)) = \sum_{i=1}^{\infty} u_i(x,t)^2,$$

respectively.

In the stochastic Galerkin projection, (2.1) is truncated to a finite number P terms, and we set

$$u(x,t,\xi) \approx u^P(x,t,\xi) = \sum_{i=0}^{P-1} u_i(x,t)\Psi_i(\xi).$$

The approximate solution u^P converges to the exact solution u as $P \to \infty$ in the L_2 norm.

Hyperbolic problems exhibit sharp gradients and shocks, for which polynomial representations are prone to fail, see e.g. [7, 8]. For robustness, localized wavelet basis functions are used. Consider the mother wavelet function defined by

$$\psi^W(y) = \begin{cases} 1 & 0 \le y < \frac{1}{2} \\ -1 & \frac{1}{2} \le y < 1 \\ 0 & \text{otherwise} \end{cases}. \tag{2.2}$$

Based on (2.2) we get the wavelet family

$$\psi^W_{j,k}(y) = 2^{j/2}\psi^W(2^j y - k), \qquad j = 0,1,...; \quad k = 0,...,2^{j-1},$$

Given the probability measure of the basis functional variable ξ with cumulative density function F_ξ, define the basis functions

$$W_{j,k}(\xi) = \Psi^W_{j,k}(F_\xi(\xi))$$

Adding the basis function $W_0(y) = 1$ in $y \in [0,1]$ and concatenating the indices j and k into $i = 2^j + k$, we can represent any second order random variable $u(x,t,\xi)$ as

$$u(x,t,\xi) = \sum_{i=0}^{\infty} u_i(x,t)W_i(\xi),$$

which is the form (2.1). For a more detailed exposition of Haar chaos representation, we refer to [9].

3. Two-phase flow problem

We assume two phases with volume fractions α and β on the domain $x \in [0,1]$, governed by the advection equation

$$\frac{\partial}{\partial t}\alpha + v\frac{\partial}{\partial x}\alpha = 0 \tag{3.1}$$

$$\beta = 1 - \alpha, \tag{3.2}$$

where v is the advective velocity. The Euler equations determine the conservation of masses $\alpha\rho_\alpha$ and $\beta\rho_\beta$, momentum ρv, and total energy E of the two phases through

$$\frac{\partial}{\partial t}\begin{bmatrix}\alpha\rho_\alpha\\ \beta\rho_\beta\\ \rho v\\ E\end{bmatrix}+\frac{\partial}{\partial x}\begin{bmatrix}\alpha\rho_\alpha v\\ \beta\rho_\beta v\\ \rho v^2+p\\ (E+p)v\end{bmatrix}=0, \tag{3.3}$$

We assume pressure p given by the perfect gas equation of state

$$p=\frac{E-\frac{1}{2}\rho v^2}{\frac{\alpha}{\gamma^{\alpha-1}}+\frac{\beta}{\gamma^{\beta-1}}},$$

and investigate the Riemann problem defined by the initial condition

$$(\alpha,\ \beta,\ \alpha\rho_\alpha,\ \beta\rho_\beta,\ \rho v,\ E)^T=\begin{cases}(1,\ 0,\ 1,\ 0,\ 0,\ 2.5)^T & x<0.5+\sigma\xi\\ (0,\ 1,\ 0,\ 0.125,\ 0,\ 0.25)^T & x>0.5+\sigma\xi\end{cases}, \tag{3.4}$$

where $\sigma=0.05$, and $\xi\in\mathcal{U}[-1,1]$.

The stochastic Galerkin formulation of the two-phase problem is obtained by multiplying (3.1) and (3.3) by each one of the basis functionals $\Psi_i(\xi)$ and the weight function of ξ, and integrating the product over the range of ξ. Initial functions are obtained by projection of (3.4) onto the basis functionals $\Psi_i(\xi)$. Truncating the order of generalized chaos to P, we get the systems

$$\frac{\partial}{\partial t}\alpha_k+\sum_{i=0}^{P}\sum_{j=0}^{P}v_i\frac{\partial}{\partial x}\alpha_j\langle\Psi_i\Psi_j\Psi_k\rangle=0 \tag{3.5}$$

$$\beta_k=\delta_{k0}-\alpha_k, \tag{3.6}$$

and

$$\frac{\partial}{\partial t}\begin{bmatrix}(\alpha\rho_\alpha)_k\\ (\beta\rho_\beta)_k\\ (\rho v)_k\\ E_k\end{bmatrix}+\frac{\partial}{\partial x}\begin{bmatrix}\sum_{i=0}^{P}\sum_{j=0}^{P}(\alpha\rho_\alpha)_i v_j\langle\Psi_i\Psi_j\Psi_k\rangle\\ \sum_{i=0}^{P}\sum_{j=0}^{P}(\beta\rho_\beta)_i v_j\langle\Psi_i\Psi_j\Psi_k\rangle\\ \sum_{i=0}^{P}\sum_{j=0}^{P}(\rho v)_i v_j\langle\Psi_i\Psi_j\Psi_k\rangle+p_k\\ \sum_{i=0}^{P}\sum_{j=0}^{P}(E_i+p_i)v_j\langle\Psi_i\Psi_j\Psi_k\rangle\end{bmatrix}=0, \tag{3.7}$$

for $k=0,...,P$. Generalized chaos expansions for e.g. the pressure can be updated from the chaos expansions of the conservative variables, and then be plugged into the fluxes.

Despite the seemingly simple nature of the initial condition, the generalized chaos series of the initial condition has an infinite number of non-zero terms. Thus, stochastic truncation error is an issue already at $t=0$.

4. Numerical method

MUSCL-type flux limiting [10] is used for the reconstruction of the left and right states of the flux. For the advection of the volume fractions, Roe's flux is used, and fourth-order Runge-Kutta is used for the time integration. For the conservative problem (3.3), we use the HLL Riemann solver introduced by Harten*et al.* [11],

$$F_{HLL}=\begin{cases}f_L & \text{if } 0\le S_L\\ \frac{S_R f_L-S_L f_R+S_L S_R(U_R-U_L)}{S_R-S_L} & \text{if } S_L\le 0\le S_R\\ f_R & \text{if } 0\ge S_R\end{cases},$$

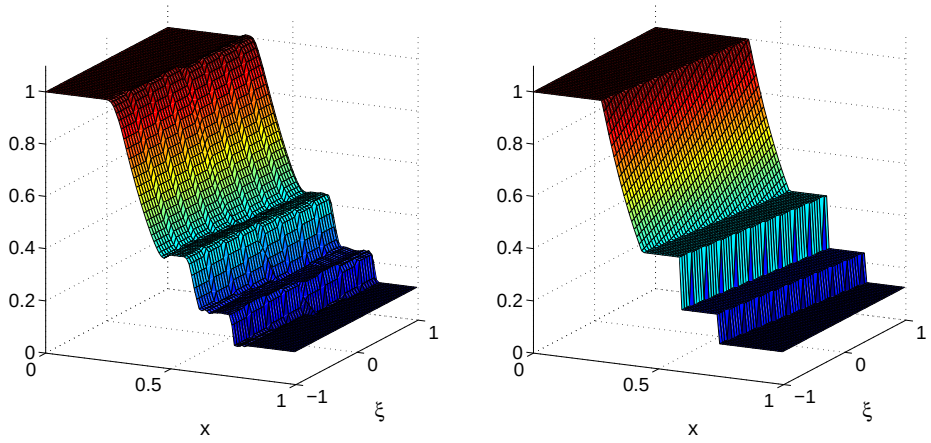

(a) Computed density, 8 wavelets. (b) Exact density.

FIGURE 1. Density as a function of x and ξ, $t = 0.15$.

where S denotes the fastest signal velocities. These are taken as estimates of the maximum and minimum eigenvalues of the Jacobian of the flux. In the deterministic case, the eigenvalues of the Jacobian are known analytically, so the method is inexpensive. For the stochastic Galerkin system, analytical expressions are not available, and numerical approximations of the eigenvalues are used instead.

The HLL-flux approximates the solution by assuming three states separated by two waves. In the deterministic case, this approximation is known to fail in capturing contact discontinuities and material interfaces [12]. The stochastic Galerkin system is a multi-wave generalization of the deterministic case, and similar problems in capturing missing waves are expected. However, the robustness and simplicity of the HLL-solver makes it a potentially more suitable choice compared to other Riemann solvers that are theoretically more accurate, but also more sensitive to ill-conditioning of the system matrix.

5. Results

The exact solution of the test problem is known analytically for any given value of the stochastic variable ξ. Thus, we can obtain the exact statistics to arbitrary accuracy by averaging the exact Riemann solutions over a large number of realizations of ξ.

Figure 1 shows the density at $t = 0.15$, computed by the stochastic Galerkin method (left) and the exact solution (right). Quantities of interest, e.g. means and variances can be computed from the stochastic Galerkin solution. The solution does not converge pointwise in ξ, but Fig. 1 gives an indication about what can be expected from quantities of interest that result from integration over ξ. For instance, the smearing (in space) of the contact surface is visible and would not vanish with refinement of the stochastic space. The dissipative effect is due to the spatial discretization, i.e. the HLL flux. Figure 2 depicts the convergence of the density with the order of generalized wavelet chaos. Higher resolution in the stochastic dimension does not change the resolution in space.

Figure 3 shows that the stochastic Galerkin method effectively captures the expectations of the variables. However, the variances are not as accurately captured as the

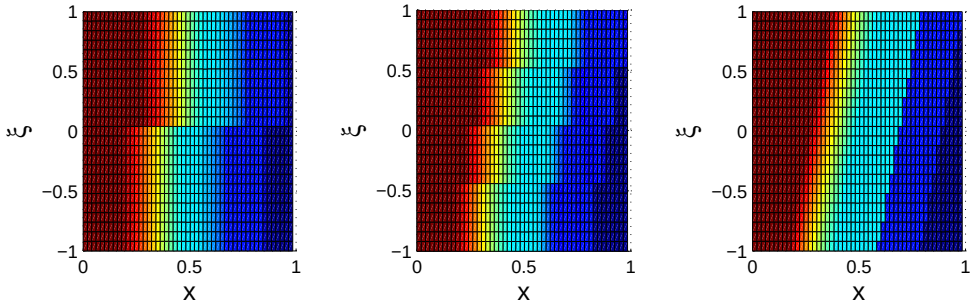

(a) Density, $P = 2$. (b) Density, $P = 4$. (c) Exact density.

FIGURE 2. Convergence of density with order of wavelet chaos, $t = 0.2$, $\sigma = 0.2$.

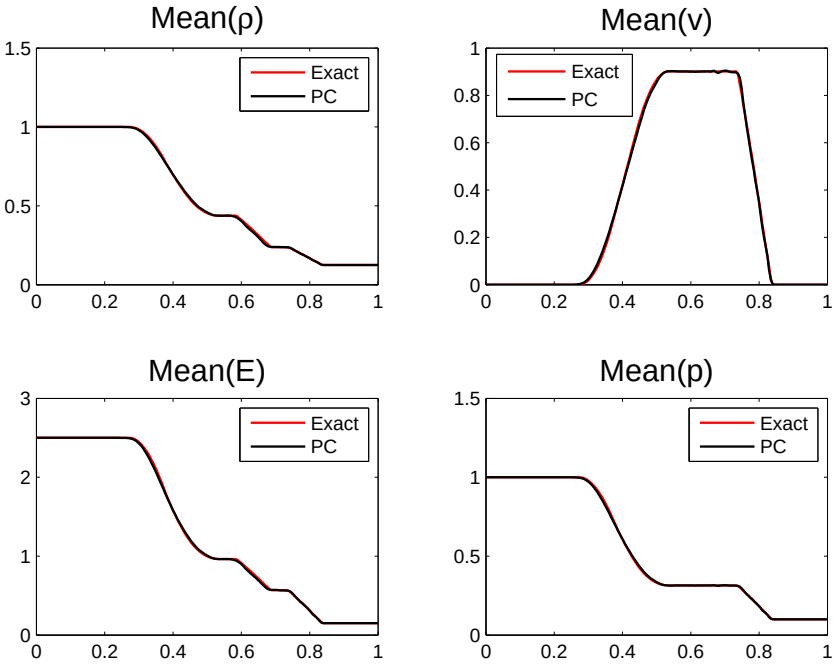

FIGURE 3. Means at $t = 0.15$, $m = 200$ grid points, 8 wavelets.

expectations, see Fig. 4. The reason and possible remedies for the underestimate of the variances will be discussed below.

The stochastic Galerkin method uses similar flux functions and flux limiters as the deterministic solver. Therefore, the stochastic Galerkin solution and Monte Carlo simulation, which are constructed as a weighted ensemble of deterministic solutions, suffer from similar problems in terms of convergence to the exact solution. As can be seen in Fig. 5(a), the numerical method underestimates the variance corresponding to uncertainty in the location of expansion region and contact discontinuity of the density. It is well-known that the HLL-flux fails to capture the contact discontinuity for the determinis-

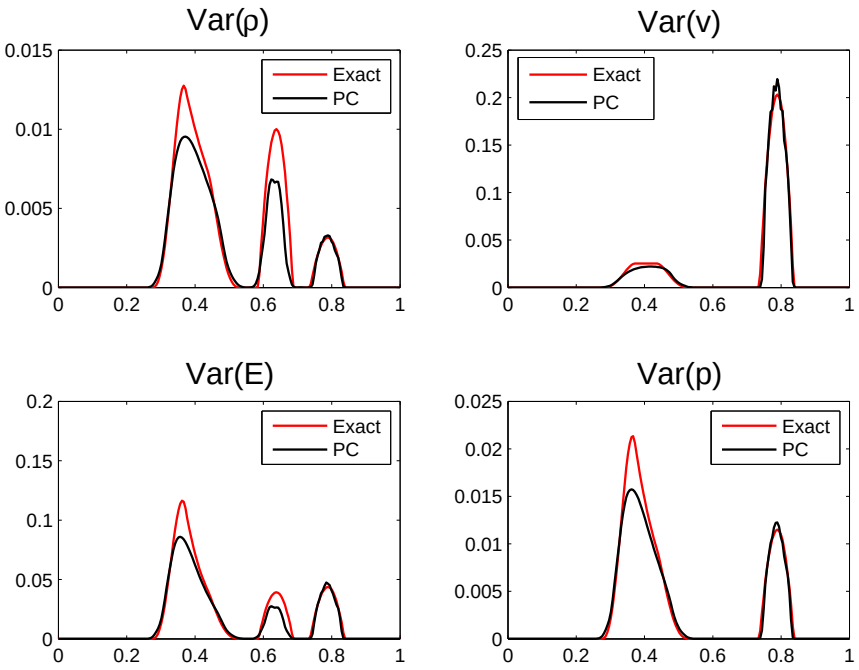

FIGURE 4. Variances at $t = 0.15$, $m = 200$ grid points, 8 wavelets.

tic case, and this also holds for the stochastic Galerkin problem. With increasing order of wavelet chaos, the stochastic Galerkin solution converges to statistics that are not equal to those of the exact solution. The same is true for Monte Carlo simulations with the deterministic HLL-solver.

Figure 6 shows that the convergence of variance and expectation of density in the discrete l_2-norm becomes saturated both for Monte Carlo simulations, Fig. 6(a), and the stochastic Galerkin method, Fig. 6(b). Each of the deterministic solves introduces an error in the Monte Carlo simulation. The error of a single deterministic solution, the density at $t = 0.15$, is shown in Fig. 7. This error is accumulated and averaged in Monte Carlo simulations, resulting in a bias in the statistics of interest.

5.1. *Computational cost*

The computational cost of the stochastic Galerkin method increases exponentially with the order of wavelet chaos. Figure 8(a) shows the exponentially increasing computational cost for different orders of wavelet chaos expansion, relative to the cost of a zeroth order wavelet chaos expansion. As a qualitative comparison, Fig. 8(b) shows the cost of Monte Carlo simulation as a function of the number of samples, relative to a single deterministic simulation. Due the exponential growth in computational time with the order of chaos expansion, uncertainty representations with coefficients with fast decay are essential to make larger problems computationally feasible. Long-time integration would require a time-adaptive generalized chaos basis to capture the transition of the probability density of the flow. Another possible means to achieve reduced computational cost is to discretize the stochastic domain (stochastic multi-elements) to decouple the system

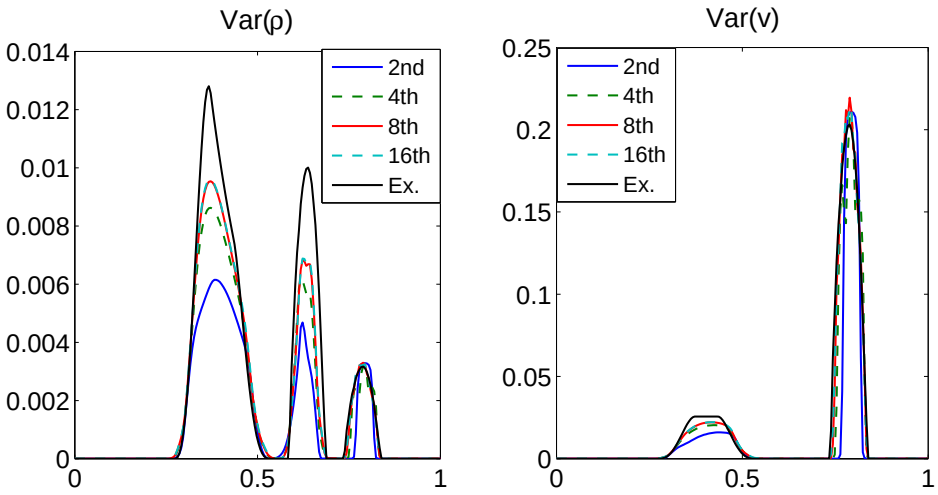

(a) Variances of density for 2, 4, 8, 16 wavelets and exact solution.

(b) Variances of velocity for 2, 4, 8, 16 wavelets and exact solution.

FIGURE 5. Convergence of variances with order of wavelet chaos.

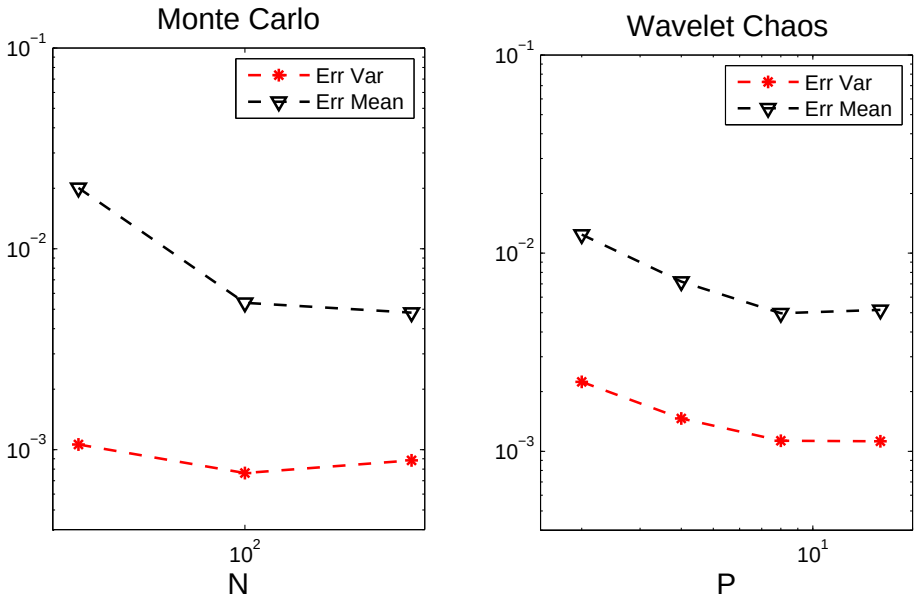

(a) Error norms for variance and mean of density using Monte Carlo.

(b) Error norms for variance and mean of density using wavelet chaos.

FIGURE 6. Comparison of errors between Monte Carlo and wavelet chaos solutions.

matrix. A low-order stochastic Galerkin method could be used for each element of the stochastic space separately.

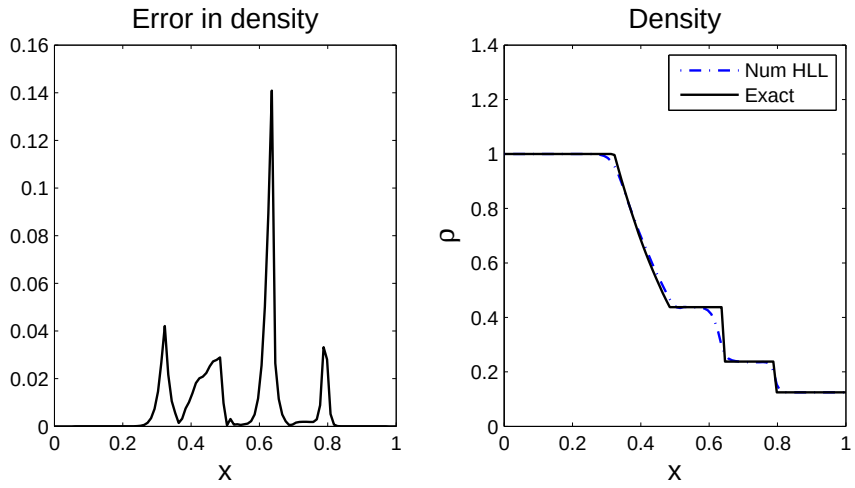

FIGURE 7. $|\rho - \rho_{exact}|$ (left) and ρ (right) at $t = 0.15$, $m = 100$ grid points.

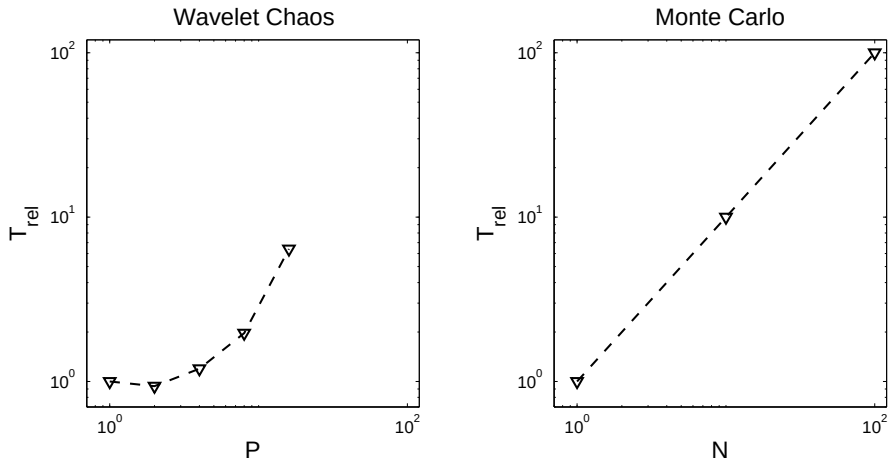

(a) Computational cost with increasing order of wavelet chaos.

(b) Computational cost with increasing number ofMonte Carlo samples.

FIGURE 8. Computational cost for wavelet chaos and Monte Carlo simulation.

6. Conclusions

The stochastic Galerkin solver shares qualitative features of the deterministic Riemann solver with HLL flux, of which it is a direct generalization. It suffers from the inability of the deterministic flux function to capture the contact discontinuity. Although the initial function was chosen to decay only slowly with the order of generalized chaos, in the present formulation, higher-order wavelet chaos would not decrease the error in computed statistics. Instead, a more accurate flux function - yet robust enough not to fail due to singularity of system matrices - is needed to increase the numerical accuracy and decrease the error. To this end, a solver that captures the material interface, e.g. a stochastic Galerkin generalization of the HLLC flux or the HLLE flux, and the expansion fan, will be required, see e.g. [13, 14].

For problems with multiple sources of uncertainty, the exponential growth of the com-

putational cost with the stochastic dimension is an issue. However, problem specific and time-dependent stochastic basis functions can be used to get an accurate uncertainty representation in relatively few chaos expansion terms for each stochastic dimensions. For a moderate number of sources of uncertainty, we believe that stochastic multi-phase problems are computationally feasible up to the accuracy of the numerical flux function.

Acknowledgments

Financial support has been provided by the German Research Foundation (Deutsche Forschungsgemeinschaft – DFG) in the framework of the Sonderforschungsbereich Transregio 40 and the IGSSE (International Graduate School of Science and Engineering) at Technische Universität München. The authors would like to thank Dr. Xiangyu Hu for ideas and fruitful discussions regarding the problem formulation and numerical methods.

References

[1] So, K. K., Chantrasmi, T., Hu, X. Y., Witteveen, J. A. S., Stemmer, C., Iaccarino, G. and Adams, N. A. (2010). Uncertainty analysis for shock-bubble interaction. In: *Proc. CTR Summer Program 2010*, 15–26.

[2] Haas, J. F. and Sturtevant, B. (1987). Interaction of weak shock waves with cylindrical and spherical gas inhomogeneities. *SIAM J. Fluid Mech.*, **181**, 41–76.

[3] Xiu, D. and Karniadakis, G. E. (2002). The Wiener-Askey polynomial chaos for stochastic differential equations. *SIAM J. Sci. Comp.*, **24**(2), 619–644.

[4] Deb, M. K., Babuska, I. M. and Oden, J. T. (2001). Solution of stochastic partial differential equations using Galerkin finite element techniques. *Comp. Meth. in Appl. Mech. and Eng.*, **190**(48), 6359–6372.

[5] Pettit, C. L. and Beran, P. S. (2006). Spectral and multiresolution Wiener expansions of oscillatory stochastic processes. *J. of. Sound and Vib.*, **294**, 752–779.

[6] Ghanem, R. G. and Spanos, P. (1991). *Stochastic Finite Elements: a Spectral Approach*. Springer.

[7] Le Maître, O. P., Knio, O. M., Najm, H. N. and Ghanem, R. G. (2004). Uncertainty propagation using Wiener-Haar expansions. *J. Comp. Phys.*, **197**, 28–57.

[8] Le Maître, O. P. and Knio, O. M. (2010). *Spectral Methods for Uncertainty Quantification*. Springer.

[9] Le Maître, O. P., Najm, H. N., Ghanem, R. G. and Knio, O. M. (2004). Multiresolution analysis of wiener-type uncertainty propagation schemes. *J. Comp. Phys.*, **197**, 502–531.

[10] van Leer, B. (1979). Towards the ultimate conservative difference scheme. V - A second-order sequel to Godunov's method. *J. Comp. Phys.*, **32**, 101–136.

[11] Harten, A., Lax, P. D. and van Leer, B. (1983). On Upstream Differencing and Godunov-Type Schemes for Hyperbolic Conservation Laws. *SIAM Rev.*, **25**(1), 35–61.

[12] Toro, E. (1997). *Riemann Solvers and Numerical Methods for Fluid Dynamics*. Springer.

[13] So, K. K., Hu, X. Y. and Adams, N. A. (2011). Anti-diffusion method for interface steepening in two-phase incompressible flow. *J. Comp. Phys.*, **230**, 5155–5177.

[14] Einfeldt, B. (1988). On Godunov-type methods for gas dynamics. *SIAM J. Num. Anal.*, **25**(2), 294–318.